HHS Public Access

Author manuscript

N Engl J Med. Author manuscript; available in PMC 2016 December 30.

Published in final edited form as:

N Engl J Med. 2016 June 30; 374(26): 2553–2562. doi:10.1056/NEJMoa1509342.

Cortical-Bone Fragility — Insights from sFRP4 Deficiency in Pyle's Disease

Pelin O. Simsek Kiper, M.D.[#], **Hiroaki Saito, Ph.D.**[#], **Francesca Gori, Ph.D.**[#], **Sheila Unger, M.D.**, **Eric Hesse, M.D., Ph.D.**, **Kei Yamana, Ph.D.**, **Riku Kiviranta, M.D., Ph.D.**, **Nicolas Solban, Ph.D.**, **Jeff Liu, M.D.**, **Robert Brommage, Ph.D.**, **Koray Boduroglu, M.D., Ph.D.**, **Luisa Bonafé, M.D.**, **Belinda Campos-Xavier, Ph.D.**, **Esra Dikoglu, M.D.**, **Richard Eastell, M.D.**, **Fatma Gossiel, M.D.**, **Keith Harshman, Ph.D.**, **Gen Nishimura, M.D.**, **Katta M. Girisha, M.D.**, **Brian J. Stevenson, Ph.D.**, **Hiroyuki Takita, M.D.**, **Carlo Rivolta, Ph.D.**, **Andrea Superti-Furga, M.D.**[#], and **Roland Baron, D.D.S., Ph.D.**[#]

[#] These authors contributed equally to this work.

Abstract

BACKGROUND—Cortical-bone fragility is a common feature in osteoporosis that is linked to nonvertebral fractures. Regulation of cortical-bone homeostasis has proved elusive. The study of genetic disorders of the skeleton can yield insights that fuel experimental therapeutic approaches to the treatment of rare disorders and common skeletal ailments.

METHODS—We evaluated four patients with Pyle's disease, a genetic disorder that is characterized by cortical-bone thinning, limb deformity, and fractures; two patients were examined by means of exome sequencing, and two were examined by means of Sanger sequencing. After a candidate gene was identified, we generated a knockout mouse model that manifested the phenotype and studied the mechanisms responsible for altered bone architecture.

RESULTS—In all affected patients, we found biallelic truncating mutations in *SFRP4*, the gene encoding secreted frizzled-related protein 4, a soluble Wnt inhibitor. Mice deficient in *Sfrp4*, like persons with Pyle's disease, have increased amounts of trabecular bone and unusually thin cortical bone, as a result of differential regulation of Wnt and bone morphogenetic protein (BMP) signaling in these two bone compartments. Treatment of *Sfrp4*-deficient mice with a soluble Bmp2 receptor (RAP-661) or with antibodies to sclerostin corrected the cortical-bone defect.

CONCLUSIONS—Our study showed that Pyle's disease was caused by a deficiency of sFRP4, that cortical-bone and trabecular-bone homeostasis were governed by different mechanisms, and that sFRP4-mediated cross-regulation between Wnt and BMP signaling was critical for achieving proper cortical-bone thickness and stability. (Funded by the Swiss National Foundation and the National Institutes of Health.)

Address reprint requests to Dr. Baron at the Department of Oral Medicine, Harvard School of Dental Medicine, 188 Longwood Ave., Boston, MA 02115, or at roland_baron@hms.harvard.edu; or to Dr. Superti-Furga at the Division of Genetic Medicine, Lausanne University Hospital (CHUV), 1011 Lausanne, Switzerland, or at asuperti@unil.ch.

Disclosure forms provided by the authors are available with the full text of this article at NEJM.org.

The authors' affiliations are listed in the Appendix.

OSTEOPOROSIS IS A SKELETAL DISEASE that is characterized by low bone mass, defective bone structure, and a high risk of fracture. Cortical-bone mass is a major determinant of bone strength and therefore of susceptibility to fractures. With aging, the mass of cortical bone may decrease more than the mass of trabecular bone, and fractures occurring in older persons result mostly from cortical-bone fragility. Although progress has been made in therapeutic approaches to reducing the risk of vertebral fracture (which occurs at sites rich in trabecular bone), currently available treatments do little to reduce the risk of nonvertebral fracture, which results mostly from cortical-bone fragility.[1-3]

Pyle's disease (Online Mendelian Inheritance in Man [OMIM] number, 265900) was described in 1931 by Edwin Pyle, an orthopedic surgeon in Connecticut, as a "case of unusual bone development"; it was described again in 1933, by the German radiologist Max Cohn, as "spongious hypertrophy of bone." Pyle's disease is characterized by long bones with wide and expanded trabecular metaphyses, thin cortical bone, and bone fragility.[4-7] Fractures are common in Pyle's disease, and fracture lines usually go through the abnormally wide metaphyses, revealing their fragility. We considered that unlike other mendelian disorders that affect overall bone density,[8] Pyle's disease seems to be a disorder of bone architecture, and an understanding of its pathogenesis might offer insights into cortical-bone homeostasis.

We evaluated four patients with Pyle's disease, by means of exome sequencing or Sanger sequencing, to identify the genetic basis for the disorder. After a candidate causal gene was identified, we studied a knockout mouse model to determine the role of the gene in the pathogenesis of Pyle's disease, in skeletal development and homeostasis, and in determining the strength of trabecular and cortical bone, as well as to test methods of treatment.

METHODS

PATIENTS

Patients 1 and 2 were a brother and sister who were referred for skeletal deformity at 16 and 14 years of age, respectively. The parents were first-degree cousins originating from Turkey; they were healthy and of normal height. The motor and mental development of Patient 1 were normal, and his height was in the upper range of normal. Tooth eruption was delayed, starting at the age of 1 year and finishing only at 7 years of age. The deciduous teeth failed to shed. Genu valgum was noted when the patient was 7 years of age and was progressive. No pain or muscular weakness was reported. He had two fractures after minimal trauma: the left radius at 7 years of age and the right femur at 17 years of age after orthopedic surgery for valgus correction. At 16 years of age, his height was 177 cm (75th percentile), his weight 60 kg (25th to 50th percentile), his head circumference 52 cm (>2 SD below the mean for his age), and his arm span 181 cm. A radiographic survey showed disturbed modeling of the long bones, with wide metaphyses and thin cortexes, and an absence of paranasal sinuses — findings consistent with Pyle's disease (Fig. 1A and 1B).[4,6] Bone mineral densitometry (conducted by means of fan beam dual-energy x-ray absorptiometry [DXA] on a GE Lunar Prodigy machine) of the lumbar spine (L1 to L4) and proximal femur revealed z scores of −2.7 and −1.1, respectively. The levels of calcium, phosphate, alkaline phosphatase, vitamin

D, and parathyroid hormone in plasma or serum were normal (Table S1 in the Supplementary Appendix, available with the full text of this article at NEJM.org).

Patient 2, the younger sister of Patient 1, had dental findings similar to those of her brother. She did not have bone fractures, walking difficulty, joint pain, or muscular weakness. At 14 years of age, her height was 172 cm (>97th percentile), her weight 51 kg (50th percentile), her head circumference 50 cm (>2 SD below the mean for her age), and her arm span 172 cm. She had genu valgum, bilateral cubitus valgus, and limitation of extension in proximal interphalangeal joints of the second, third, fourth, and fifth fingers. The radiographic findings were similar to those in her elder brother and were consistent with Pyle's disease (Fig. S1 in the Supplementary Appendix).[4,6] Bone mineral densitometry of the lumbar spine (L1 to L4) and proximal femur revealed z scores of −2.1 and −1.4, respectively. The serum levels of calcium, phosphate, alkaline phosphatase, vitamin D, and parathyroid hormone were normal; levels of bone metabolism markers are shown in Table S1 in the Supplementary Appendix.

The unaffected parents of Patients 1 and 2 and an unaffected younger brother consented to undergo a clinical and radiographic workup. The results of routine blood chemical tests were normal; levels of bone metabolism markers were also within age-specific reference ranges (Table S1 in the Supplementary Appendix). Skeletal radiographs showed a mild tubulation defect of the long bones, as has been observed previously in obligate heterozygotes for Pyle's disease (Fig. S2 in the Supplementary Appendix).[4,6]

Patient 3 was a 58-year-old man who was evaluated for a possible fracture after a workplace accident. His height was 173 cm, and his weight was 72 kg; both measures were between the 50th and the 75th percentile for Japanese men. He was from Kyushu island, a region with a relatively high level of consanguinity. No details of his early medical history are known. Fractures were noted in the tibia, but the tibia also had a highly abnormal shape and structure that prompted additional radiographic evaluation. The findings were considered typical for Pyle's disease (Fig. 1D, and Fig. S1 in the Supplementary Appendix).[4,6]

Patient 4 was a boy from India. His biologic parents were unknown. He was examined at the age of 3 years 6 months because of progressive genu valgus deformity that had developed after he started walking. Apart from the leg deformity, he was in good health; his height was in the 10th percentile, and there was no history of fractures. His primary dentition looked normal. Radiographs showed the metaphyseal tubulation defect, chalk-like appearance of the bone, and lack of cortical bone that are typical of Pyle's disease (Fig. S1 in the Supplementary Appendix).[4,6]

OVERSIGHT AND LABORATORY STUDIES

Informed consent was obtained from the patients, their parents, or both with the use of the consent forms of the Hacettepe University Hospital (Ankara, Turkey), the Manipal University Hospital (Manipal, India), or the Lausanne University Hospital (Lausanne, Switzerland). The genetic study was conducted with the approval of the ethics commission of the Lausanne University Hospital. In brief, we sequenced the exomes of Patients 1 and 2; in addition, the exons of *SFRP4* in Patients 3 and 4 were sequenced by means of Sanger

sequencing. Details of the laboratory procedures, bioinformatics filtering, and prioritization of variants are provided in the Supplementary Appendix. We did not include any other patients with Pyle's disease in the analysis.

We obtained two independent lines of knockout mice, one from Procter & Gamble and one from Lexicon; both lines had disruption of the first exon of *Sfrp4* and had the same phenotype. Full details regarding the generation of mouse models, skeletal phenotyping, ex vivo and in vitro studies, and in vivo treatment with the bone morphogenetic protein (BMP) inhibitor, RAP-661, and sclerostin antibodies are provided in the Supplementary Appendix.

RESULTS

IDENTIFICATION OF *SFRP4* MUTATIONS

Filtering of the exome-sequencing data from Patients 1 and 2 (Table S2 in the Supplementary Appendix) resulted in the retention of three homozygous variants: one in the complement component 9 gene (*C9*), one in *DAB2*, and a single-nucleotide insertion predicted to result in a frame-shift with a premature stop codon (c.498_499insG; p.Asp167Glyfs*3) in *SFRP4*, the gene encoding secreted frizzled-related protein 4 (sFRP4) (Fig. 1F and 1I). The *SFRP4* variant stood out because it affects a protein involved in a pathway that is highly relevant to bone homeostasis — that is, the Wnt-signaling pathway.[9] *SFRP4* polymorphisms had been linked to bone mineral density in genome-wide association studies,[10-13] and *SFRP4* had been suggested as a candidate gene for craniotubular disorders, although no pathogenic mutation had been identified.[14] Segregation analysis confirmed heterozygosity in both parents and in the unaffected brother.

In Patient 3, Sanger sequencing of *SFRP4* in genomic DNA revealed homozygosity for a different point mutation (c.694C→T; p.Arg232*) that was predicted to result in a premature stop codon with truncation of the protein (Fig. 1G and 1I). In Patient 4, we found a homozygous deletion of seven nucleotides (c.481_487delGTACAGG; p.Val161Lysfs*11) that was predicted to result in a short stretch of 10 missense amino acids followed by a premature stop codon (Fig. 1H); the predicted effect of this mutation at the messenger RNA (mRNA) level was remarkably similar to that of the mutation that was found in Patients 1 and 2. Thus, the observed mutations in all four patients were predicted to result in premature stop codons with truncation of the sFRP4 protein. These mutations could result in either nonsense-mediated mRNA decay or, if the mRNA were translated, the synthesis of a protein lacking a large portion of the netrin-like domain, which is necessary for positioning of sFRP4[15] and for Wnt inhibition.[16] Quantitative polymerase-chain-reaction analysis of fibroblast mRNA from Patient 2 revealed a severe reduction in *SFRP4* mRNA (Fig. S3 in the Supplementary Appendix), which suggests that the c.498_499insG mutation results in nonsense-mediated mRNA decay.

MARKERS OF BONE TURNOVER

We assayed plasma levels of osteocalcin, procollagen type 1 N-terminal propeptide (P1NP), and bone-specific alkaline phosphatase as markers of bone formation, carboxy-terminal collagen cross-links as a marker of bone resorption, and osteoprotegerin and sclerostin in all

members of Family 1 (Table S1 in the Supplementary Appendix). The P1NP levels exceeded those of age-related and puberty-related control values in both affected family members, possibly resulting from an increased rate of type I collagen synthesis and deposition. Osteocalcin levels were also higher than reference values. The levels of bone-specific alkaline phosphatase were elevated in both affected family members and in the heterozygous brother. Together, the three osteoblast-derived metabolites seem to indicate a particularly active bone deposition process. The levels of carboxy-terminal collagen crosslinks were normal, which suggested a normal bone resorption rate at the systemic level. Levels of osteoprotegerin and sclerostin were also in the normal ranges.

BONE FINDINGS IN MICE LACKING *SFRP4*

In *Sfrp4*-null mice (Fig. S4A, S4B, and S4C in the Supplementary Appendix), levels of systemic bone markers were not substantially altered, and serum levels of calcium, phosphate, and 1,25-dihydroxy-vitamin D were normal,[17] despite substantial and diametrically opposed changes in cortical bone versus trabecular bone. Radiographs (Fig. 2A) showed expanded metaphyses with thin cortical bone in femora and tibiae when the mice were as young as 2 weeks of age — changes that were remarkably similar to those observed in the patients (Fig. 1). Microcomputed tomography analysis of femora from *Sfrp4*-null mice confirmed the presence of thin cortexes, as compared with those of wild-type littermates (Fig. 2B); thin cortical bone was also found in the calvaria, indicating that the cortex in long bones and in the calvaria are equally affected by the absence of *Sfrp4*. Histologic examination of 10-week-old mice revealed expanded metaphyses surrounded by thin cortexes (Fig. 2C). Histomorphometric analysis confirmed a disturbed microarchitecture of the skeleton, in homozygous mice and in heterozygous mice: specifically, there was a gene dosage–dependent increase in trabecular-bone volume and bone-formation rates (Fig. 2C) in addition to a gene dosage–dependent reduction in cortical-bone thickness in long bones (Fig. 2C). This was accompanied by a reduction in mechanical strength measured at the diaphysis. The rates of periosteal and endocortical mineral apposition were equally reduced in adult mice, whereas the width of the bones at midshaft was increased (Fig. 2C). Altogether, these results suggest that the absence of *Sfrp4* led to increased trabecular bone, reduced cortical-bone thickness, and failure of bone modeling during growth, resulting in wider bones with thinner and mechanically inadequate cortexes. The findings are similar to those in Pyle's disease and confirm a pathophysiological mechanism involving vigorous formation of trabecular bone but an impairment in the formation of cortical bone. Additional radiographs of humans and mice and other details on the bone findings are provided in Figures S1, S2, S4, and S5 and Table S3 in the Supplementary Appendix.

OSTEOBLAST, OSTEOCLASTS, AND *SFRP4* DEFICIENCY

The protein sFrp4 is a soluble Wnt decoy receptor that binds Wnt ligands and thus modulates both canonical (i.e., β-catenin–dependent) and noncanonical (i.e., β-catenin–independent) Wnt signaling.[15,19] To understand the effects of *Sfrp4* deficiency on cortical and trabecular bone, we first sought to determine whether the activation state of the Wnt-signaling pathway differs between these two compartments. Given that *Sfrp4*-null long-bone cortex and calvariae have the same phenotype (decreased thickness), we used primary calvarial osteoblasts to investigate the molecular mechanisms by which *Sfrp4* modulates

cortical bone. Similarly, because trabecular bone is intimately associated with the bone marrow compartment, we used bone marrow–derived osteoblasts to assess the effect of *Sfrp4* deficiency on trabecular bone. *Sfrp4*-null calvarial osteoblasts had activation of both canonical and noncanonical Wnt signaling, as indicated by an increase in active β-catenin and phosphorylated Jnk levels and by an increase in the expression of the canonical Wnt target gene *Axin2*; in contrast, *Sfrp4* deficiency led to activation of canonical Wnt signaling but not of noncanonical Wnt signaling in bone marrow–derived osteoblasts (Fig. 2D, and Fig. S6A in the Supplementary Appendix). This difference suggested that the reduced cortical bone thickness might result from activation of noncanonical Wnt signaling.

Expression of sclerostin, an osteocyte-derived potent Wnt inhibitor,[20-23] was markedly increased in *Sfrp4*-null calvarial osteoblasts but only mildly increased in bone marrow–derived osteoblasts (Fig. 2E), which suggests a possible explanation for this differential effect. The sclerostin gene, *Sost*, is a known target of the BMP signaling pathway,[24] and activation of BMP signaling has been shown to lead to thin bone cortex.[25] Therefore, we sought to determine whether changes in BMP expression, BMP signaling, or both in response to activated noncanonical Wnt signaling might be contributing to the cortical phenotype in *Sfrp4*-null mice. Activation of noncanonical signaling by Wnt5a in the osteoblast cell line MC3T3-E1 increased *Bmp2* mRNA expression (Fig. 2F); this effect was blocked by the addition of sFrp4 (Fig. 2F) and enhanced in the absence of *Sfrp4* (Fig. 2G). In addition, sFrp4 inhibited the Wnt5a-dependent activation of the BMP-responsive *Id–luc* reporter gene, as did Noggin and RAP-661, both of which are inhibitors of BMP signaling (Fig. S6B in the Supplementary Appendix).[19,20] This effect of sFrp4 was blocked by Jnk inhibitors, whereas Wnt3a, a classic canonical Wnt ligand, did not alter the activation of the *Id–luc* reporter gene; this confirms that activation of BMP signaling depends on the noncanonical branch of Wnt signaling. Thus, noncanonical Wnt signaling activates the BMP pathway, and sFrp4 inhibits this activation. *Sfrp4* deficiency is thus expected to result in enhanced BMP signaling. Accordingly, expression of *Bmp2* and of its target gene *Id2*, as well as phosphorylation of Smad1, Smad5, and Smad8, were increased in calvarial osteoblasts derived from *Sfrp4*-null mice but not in bone marrow–derived osteoblasts derived from *Sfrp4*-null mice (Fig. 2H, and Fig. S6C and S6D in the Supplementary Appendix), a finding that supports the hypothesis of compartment-specific effects.

Both canonical and noncanonical Wnt signaling cascades also affect osteoclastogenesis and bone resorption.[9,26-30] In *Sfrp4*-null mice, the number of osteoclasts was normal in trabecular bone (Table S3 in the Supplementary Appendix) but significantly increased along the diaphyseal endocortical surface (Fig. S7A in the Supplementary Appendix). In growing (8-day-old) *Sfrp4*-null mice, the number of osteoclasts along the periosteum was reduced, although not significantly (mean [±SE], 2.0±0.3 osteoclasts per periosteal perimeter in *Sfrp4*-null mice vs. 2.4±0.3 osteoclasts per periosteal perimeter in wild-type mice; six mice per genotype were analyzed), and was consistently increased along the endosteum (6.3±0.8 osteoclasts per endosteal perimeter in *Sfrp4*-null mice vs. 4.7±0.7 osteoclasts per endosteal perimeter in wild-type mice; six mice per genotype were analyzed), which may explain the abnormal shape and metaphyseal expansion. Together with the decreased cortical-bone formation (Fig. S5 in the Supplementary Appendix), the increase in endocortical bone resorption would be expected to contribute to the thinning of cortical bone in *Sfrp4*-null

adult mice. Increased osteoclastogenesis is consistent with an increase in the ratio of *Rankl* expression to *Opg* expression (Fig. S7B in the Supplementary Appendix). These findings show that sFrp4 acts on osteoblasts to suppress endocortical osteoclastogenesis by binding to noncanonical Wnts (such as Wnt5a) and preventing activation of BMP signaling in the cortex.

REVERSING THE EFFECTS OF *SFRP4* DEFICIENCY

We therefore used RAP-661 to inhibit the BMP pathway in vivo.[31] Pharmacologic inhibition of the BMP pathway increased cortical-bone thickness in wild-type mice and, in mice that were heterozygous for an *Sfrp4* mutation, restored the cortical-bone mass to the level found in vehicle-treated wild-type mice (Fig. 2I), while further increasing the mass of trabecular bone. In addition, RAP-661 treatment significantly improved the thickness and bone mineral density of calvarial bones of heterozygous mice. When administered from an early age, this treatment led to an improved bone shape, partially reversing the bone-modeling defect (Fig. 2I). We observed a similar effect on the bone mineral density of the tibia mid-shaft cortical region. The finding that treatment with RAP-661 reduced the endogenous expression of sclerostin both in wild-type mice and in heterozygous mice suggested the possibility of using a sclerostin-neutralizing antibody to block the effects of sclerostin directly.[31-33] Inactivation of sclerostin in vivo restored the cortical bone thickness in *Sfrp4*-null mice and significantly reduced bone diameter (Fig. 2J). Additional pharmacologic data are available in Figure S8 and Tables S4 and S5 in the Supplementary Appendix.

DISCUSSION

Although cortical-bone fragility is a major contributor to osteoporotic nonvertebral fractures, little is known about the specific regulation of cortical-bone thickness and density. Moreover, current antiosteoporosis therapies have a greater effect on trabecular bone than on cortical bone; relative changes in trabecular-bone mass in response to treatment and as measured by DXA, and thereby the reduction of the risk of vertebral fractures, are of greater magnitude than are those of cortical-bone and nonvertebral fractures. We explored the mechanisms that cause Pyle's disease, a genetic disorder that is characterized by cortical-bone fragility, limb deformity, and fractures, in an effort to understand the mechanisms by which cortical-bone homeostasis is regulated. In previous studies, genetic bone disorders have provided insights into the mechanisms by which bone is formed and maintained.[9,34,35] On radiographs of patients with Pyle's disease, the metaphyses of tubular bones are widened (their shape is similar to that of an oar), the bone cortex is either reduced to a barely visible line or absent altogether, and the central rarefaction of trabecular bone tissue is lacking; instead, the metaphyses seem to be composed of homogeneous trabecular bone.[5,6] The radiographic findings in our study suggested a vigorous formation of trabecular bone and an impairment in the formation or homeostasis of cortical bone, and the abnormal shape suggested a failure of the remodeling process that occurs in cortical bone during growth.

The genetic studies provided evidence that recessive mutations in *SFRP4* are a cause of Pyle's disease. We therefore explored the cellular mechanisms of the abnormal bone architecture in *Sfrp4*-null mice. The mouse model reproduced the human phenotype to a

remarkable degree. We showed that the phenotype was due to the differential regulation of Wnt signaling and BMP signaling (Fig. S9 in the Supplementary Appendix). Whereas deletion of *Sfrp4* activated predominantly canonical Wnt signaling in trabecular bone, leading to increased trabecular bone mass, both canonical and noncanonical Wnt signaling were increased in cortical bone. We went on to show that both noncanonical Wnt and BMP signaling in cortical bone prevented cortical-bone formation and had to be down-regulated by sFRP4 to allow for proper cortex thickness and strength.

Our results also highlight critical limitations of the most commonly used tools for the diagnosis and evaluation of skeletal diseases. For example, DXA measurements that are widely used to predict fractures are often discordant between cortical (femur) and trabecular (spine) bone sites, leaving clinicians in a quandary about whether to treat. This is further illustrated in our study, in which, despite the presence of profoundly altered bone structure involving increased trabecular bone and extremely thin cortexes, neither classic measurements of bone mineral density nor biochemical markers were reliable indicators of risk. The decreased bone mineral density must reflect the very thin cortex, but it fails to indicate whether the density of trabecular bone is normal or increased. Similarly, markers of bone formation are systemically increased, whereas markers of bone resorption are unchanged in these patients, which reflects the status of the trabecular bone but not of cortical bone. In the future, high-resolution quantitative computed tomography and the development of cortical-bone markers, such as periostin,[36,37] may allow an assessment of these two bone compartments, as well as stratification of the two bone compartments with respect to risk prediction.

In summary, we showed that Pyle's disease was caused by a genetic deficiency in sFRP4, that there were differences in the homeostasis of cortical bone versus trabecular bone, and that these processes might be specifically modulated by pharmacologic interventions.

Supplementary Material

Refer to Web version on PubMed Central for supplementary material.

Acknowledgments

Supported by the Swiss National Foundation, the Leenaards Foundation in Lausanne, the Scientific and Technological Research Council of Turkey (TUBITAK program 2219), a grant from the Japan Society for the Promotion of Science (to Dr. Saito), and a grant from the National Institute of Arthritis and Musculoskeletal and Skin Diseases, National Institutes of Health (R01AR064724 to Dr. Baron).

We thank Chris Paszty from Amgen for providing the sclerostin antibodies and advice on their use, Matthew Warman from Children's Hospital Boston and Harvard Medical School and Matthias Wagner from the Zurich University Hospital for discussions, and Andreas Grauer and George Sabatakos for their help in initiating this project.

APPENDIX

The authors' affiliations are as follows: the Center for Molecular Diseases (P.O.S.K., L.B., B.C.-X., E.D.), Medical Genetics Service (S.U.), and Department of Pediatrics (A.S.-F.), Lausanne University Hospital, the Genomic Technologies Facility, Center for Integrative

Genomics (K.H.), and Department of Computational Biology, Unit of Medical Genetics (C.R.), University of Lausanne, and the Swiss Institute of Bioinformatics (B.J.S.) — all in Lausanne, Switzerland; the Unit of Pediatric Genetics, Department of Pediatrics, Hacettepe University Medical Faculty, Ankara, Turkey (P.O.S.K., K.B.); Harvard School of Dental Medicine, Department of Oral Medicine, Infection, and Immunity (H.S., F. Gori, E.H., K.Y., R.K., R. Baron), and Harvard Medical School, Department of Medicine, Endocrine Unit, Massachusetts General Hospital (R. Baron) — both in Boston; Acceleron Pharma, Cambridge, MA (N.S.); Lexicon Pharmaceuticals, The Woodlands, TX (J.L., R. Brommage); Academic Unit of Bone Metabolism, Metabolic Bone Centre Northern General Hospital, Sheffield, United Kingdom (R.E., F. Gossiel); the Department of Radiology and Medical Imaging, Tokyo Metropolitan Kiyose Children's Hospital, Kiyose (G.N.), and the Department of Orthopedics, National Hospital Organization Saga Hospital, Saga (H.T.) — both in Japan; and the Department of Medical Genetics, Kasturba Medical College, Manipal University, Manipal, India (K.M.G.).

REFERENCES

1. Baron R, Hesse E. Update on bone anabolics in osteoporosis treatment: rationale, current status, and perspectives. J Clin Endocrinol Metab. 2012; 97:311–25. [PubMed: 22238383]
2. Black DM, Rosen CJ. Postmenopausal osteoporosis. N Engl J Med. 2016; 374:254–62. [PubMed: 26789873]
3. Zebaze RM, Ghasem-Zadeh A, Bohte A, et al. Intracortical remodelling and porosity in the distal radius and post-mortem femurs of women: a cross-sectional study. Lancet. 2010; 375:1729–36. [PubMed: 20472174]
4. Beighton P. Pyle disease (metaphyseal dysplasia). J Med Genet. 1987; 24:321–4. [PubMed: 3612703]
5. Cohn M. Konstitutionelle Hyperspongiosierung des Skeletts mit partiellem Riesenwuchs. Fortschr Röntgenstr. 1933; 47:293–8.
6. Heselson NG, Raad MS, Hamersma H, Cremin BJ, Beighton P. The radiological manifestations of metaphyseal dysplasia (Pyle disease). Br J Radiol. 1979; 52:431–40. [PubMed: 465917]
7. Pyle E. A case of unusual bone development. J Bone Joint Surg Am. 1931; 13:874–6.
8. Bonafe L, Cormier-Daire V, Hall C, et al. Nosology and classification of genetic skeletal disorders: 2015 revision. Am J Med Genet A. 2015; 167:2869–92.
9. Baron R, Kneissel M. WNT signaling in bone homeostasis and disease: from human mutations to treatments. Nat Med. 2013; 19:179–92. [PubMed: 23389618]
10. Cho YS, Go MJ, Kim YJ, et al. A large-scale genome-wide association study of Asian populations uncovers genetic factors influencing eight quantitative traits. Nat Genet. 2009; 41:527–34. [PubMed: 19396169]
11. Karasik D, Cupples LA, Hannan MT, Kiel DP. Age, gender, and body mass effects on quantitative trait loci for bone mineral density: the Framingham Study. Bone. 2003; 33:308–16. [PubMed: 13678771]
12. Lee DY, Kim H, Ku SY, Kim SH, Choi YM, Kim JG. Association between polymorphisms in Wnt signaling pathway genes and bone mineral density in post-menopausal Korean women. Menopause. 2010; 17:1064–70. [PubMed: 20613673]
13. Styrkarsdottir U, Halldorsson BV, Gretarsdottir S, et al. Multiple genetic loci for bone mineral density and fractures. N Engl J Med. 2008; 358:2355–65. [PubMed: 18445777]
14. Boudin E, Piters E, Fijalkowski I, et al. Mutations in sFRP1 or sFRP4 are not a common cause of craniotubular hyperostosis. Bone. 2013; 52:292–5. [PubMed: 23044044]
15. Kawano Y, Kypta R. Secreted antagonists of the Wnt signalling pathway. J Cell Sci. 2003; 116:2627–34. [PubMed: 12775774]

16. Bhat RA, Stauffer B, Komm BS, Bodine PV. Structure-function analysis of secreted frizzled-related protein-1 for its Wnt antagonist function. J Cell Biochem. 2007; 102:1519–28. [PubMed: 17471511]
17. Christov M, Koren S, Yuan Q, Baron R, Lanske B. Genetic ablation of sfrp4 in mice does not affect serum phosphate homeostasis. Endocrinology. 2011; 152:2031–6. [PubMed: 21427221]
18. Livak KJ, Schmittgen TD. Analysis of relative gene expression data using real-time quantitative PCR and the 2(−Delta Delta C(T)) Method. Methods. 2001; 25:402–8. [PubMed: 11846609]
19. Wawrzak D, Métioui M, Willems E, Hendrickx M, de Genst E, Leyns L. Wnt3a binds to several sFRPs in the nanomolar range. Biochem Biophys Res Commun. 2007; 357:1119–23. [PubMed: 17462603]
20. Balemans W, Ebeling M, Patel N, et al. Increased bone density in sclerosteosis is due to the deficiency of a novel secreted protein (SOST). Hum Mol Genet. 2001; 10:537–43. [PubMed: 11181578]
21. Liu Y, Rubin B, Bodine PV, Billiard J. Wnt5a induces homodimerization and activation of Ror2 receptor tyrosine kinase. J Cell Biochem. 2008; 105:497–502. [PubMed: 18615587]
22. Poole KE, van Bezooijen RL, Loveridge N, et al. Sclerostin is a delayed secreted product of osteocytes that inhibits bone formation. FASEB J. 2005; 19:1842–4. [PubMed: 16123173]
23. van Bezooijen RL, Roelen BA, Visser A, et al. Sclerostin is an osteocyte-expressed negative regulator of bone formation, but not a classical BMP antagonist. J Exp Med. 2004; 199:805–14. [PubMed: 15024046]
24. Kamiya N, Kobayashi T, Mochida Y, et al. Wnt inhibitors Dkk1 and Sost are downstream targets of BMP signaling through the type IA receptor (BMPRIA) in osteoblasts. J Bone Miner Res. 2010; 25:200–10. [PubMed: 19874086]
25. Canalis E, Brunet LJ, Parker K, Zanotti S. Conditional inactivation of Noggin in the postnatal skeleton causes osteopenia. Endocrinology. 2012; 153:1616–26. [PubMed: 22334719]
26. Glass DA II, Bialek P, Ahn JD, et al. Canonical Wnt signaling in differentiated osteoblasts controls osteoclast differentiation. Dev Cell. 2005; 8:751–64. [PubMed: 15866165]
27. Holmen SL, Zylstra CR, Mukherjee A, et al. Essential role of beta-catenin in postnatal bone acquisition. J Biol Chem. 2005; 280:21162–8. [PubMed: 15802266]
28. Wei W, Zeve D, Suh JM, et al. Biphasic and dosage-dependent regulation of osteoclastogenesis by β-catenin. Mol Cell Biol. 2011; 31:4706–19. [PubMed: 21876000]
29. Maeda K, Kobayashi Y, Udagawa N, et al. Wnt5a-Ror2 signaling between osteo-blast-lineage cells and osteoclast precursors enhances osteoclastogenesis. Nat Med. 2012; 18:405–12. [PubMed: 22344299]
30. Sen M, Chamorro M, Reifert J, Corr M, Carson DA. Blockade of Wnt-5A/frizzled 5 signaling inhibits rheumatoid synoviocyte activation. Arthritis Rheum. 2001; 44:772–81. [PubMed: 11315916]
31. Mulivor A, Solban N, Kawamoto Y, Kumar R, Seehra J, Pearsall RS. Inhibition of ALK3 (BMPRIA) signaling using RAP-661, a novel bmp antagonist, increases bone mass in ovariectomized mice. Bone. 2011; 48(Suppl 2):S98–9.
32. Li X, Warmington KS, Niu QT, et al. Inhibition of sclerostin by monoclonal antibody increases bone formation, bone mass, and bone strength in aged male rats. J Bone Miner Res. 2010; 25:2647–56. [PubMed: 20641040]
33. Padhi D, Jang G, Stouch B, Fang L, Posvar E. Single-dose, placebo-controlled, randomized study of AMG 785, a sclerostin monoclonal antibody. J Bone Miner Res. 2011; 26:19–26. [PubMed: 20593411]
34. Briggs MD, Bell PA, Wright MJ, Pirog KA. New therapeutic targets in rare genetic skeletal diseases. Expert Opin Orphan Drugs. 2015; 3:1137–54. [PubMed: 26635999]
35. Warman ML, Cormier-Daire V, Hall C, et al. Nosology and classification of genetic skeletal disorders: 2010 revision. Am J Med Genet A. 2011; 155A:943–68. [PubMed: 21438135]
36. Cheung AM, Adachi JD, Hanley DA, et al. High-resolution peripheral quantitative computed tomography for the assessment of bone strength and structure: a review by the Canadian Bone Strength Working Group. Curr Osteoporos Rep. 2013; 11:136–46. [PubMed: 23525967]

37. Kim BJ, Rhee Y, Kim CH, et al. Plasma periostin associates significantly with non-vertebral but not vertebral fractures in postmenopausal women: clinical evidence for the different effects of periostin depending on the skeletal site. Bone. 2015; 81:435–41. [PubMed: 26297442]

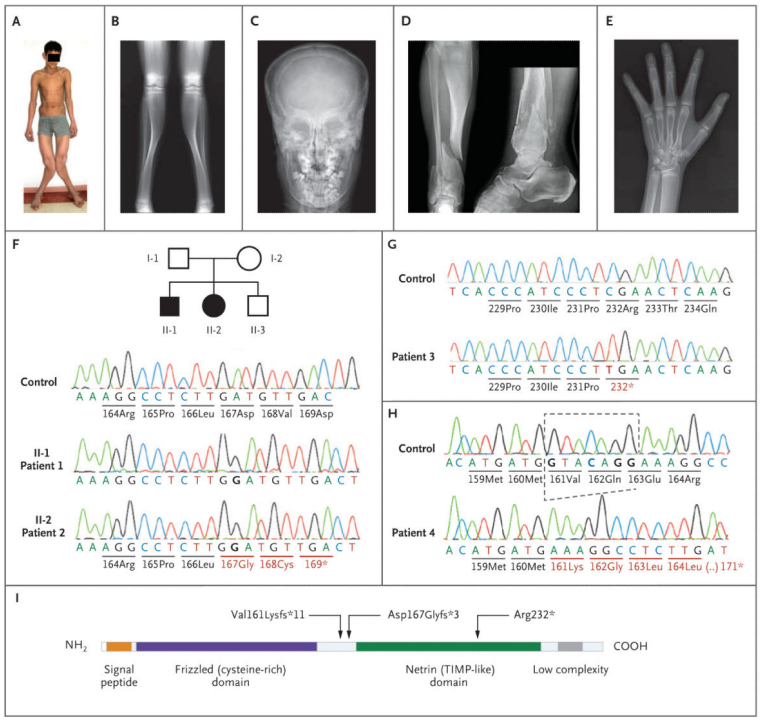

Figure 1. Clinical, Radiographic, and Molecular Findings

Panel A shows Patient 1 at 16 years of age; he had deformation of the lower limbs with marked valgus of both legs. The expanded distal femora could be easily palpated above the knees. Panel B is a radiograph of the lower limbs in Patient 1, showing expanded metaphyses of the distal femora and proximal and distal tibiae with extremely thin cortexes. The appearance of the bone at the tibial midshaft, with thicker cortex, is relatively normal. Panel C is an anteroposterior skull radiograph of Patient 2, showing expansion of the diploe. Panel D is an anteroposterior and lateral projection of the distal right tibia in Patient 3, showing changes similar to those in Panel B. In addition, two fractures run through the abnormal metaphysis, and a third fracture runs through the distal fibula. Panel E is a hand radiograph of Patient 2 at 14 years of age, showing expanded metaphyses and thin cortexes at the distal radius, as well as expansion of the distal metacarpals and (to a lesser degree) of the phalanges. Panels F, G, and H show the nucleotide sequences of *SFRP4* in controls, affected patients, and heterozygous family members. Patients 1 and 2 are homozygous for a nucleotide insertion in exon 2 (Panel F); as a result, amino acid residues 167 and 168 are replaced, and a stop codon is generated at position 169, leading to a truncated protein. Both parents and the brother are heterozygous for the insertion. Circles denote female family members, squares male family members, open symbols unaffected family members, and black symbols affected family members. Patient 3 is homozygous for a C-to-T transition that transforms codon 232 from arginine to a stop codon (Panel G). Patient 4 is homozygous for the deletion of 7 nucleotides; as a consequence, there is a stretch of 10 missense amino acids (codons 161–170), followed by a premature termination at codon 171 (Panel H). Panel I is a diagram of the sFRP4 protein, illustrating the two main domains as well as the positions of the three mutations found in the patients.

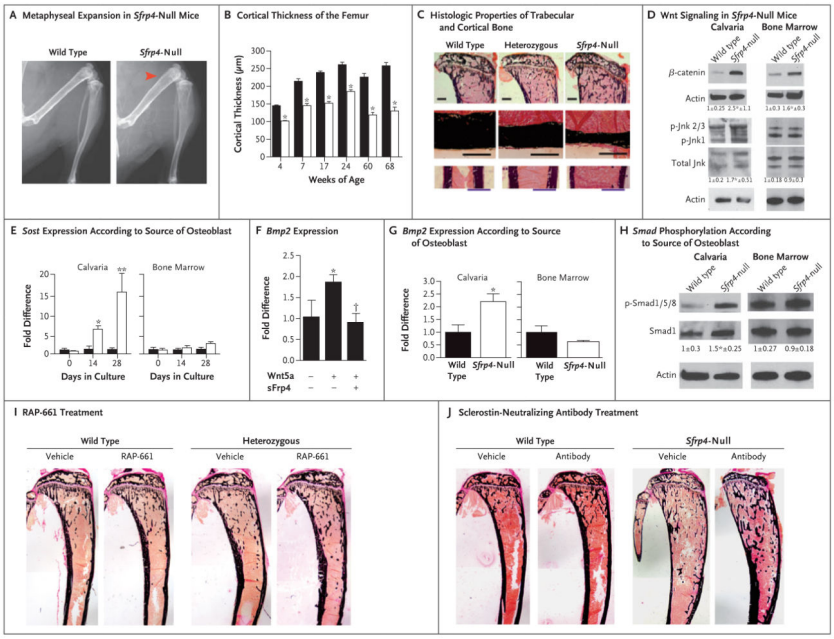

Figure 2. Functional Consequences of *Sfrp4* Deletion and Correction of the Cortical Phenotype in *Sfrp4*-Null Mice

Panel A shows representative radiographic images of wild-type and *Sfrp4*-null female littermates at 10 weeks of age. The arrowhead indicates the expanded metaphyses in the *Sfrp4*-null mice (four mice were analyzed in each genotype). Panel B shows microcomputed tomography (microCT) analysis of cortical thickness in femur midshaft of wild-type (black bars) and *Sfrp4*-null (open bars) mice at 4, 7, 17, 24, 60, and 68 weeks of age. The bars show mean values; T bars indicate standard errors. P<0.05 for the comparison with wild-type at each time point (five mice were analyzed in each genotype). Panel C shows representative histologic features of von Kossa–stained trabecular bone in proximal tibiae (top row; scale bar, 1 mm) and cortical bone in the tibial midshaft region (bottom two rows; scale bars, 300 μm) of wild-type, heterozygous, and *Sfrp4*-null mice at 10 weeks of age (five mice were analyzed in each genotype). *Sfrp4* deletion leads to increased trabecular bone, decreased cortical thickness, and increased width. Panel D shows the differential effects of *Sfrp4* deletion on canonical and noncanonical Wnt signaling in calvarial osteoblasts and bone marrow–derived osteoblasts. The total amount of active β-catenin, phosphorylated Jnk (p-Jnk), and total Jnk was assessed in calvarial osteoblasts and bone marrow–derived osteoblasts isolated from *Sfrp4*-null and wild-type littermates. Actin was used as a loading control. Fold differences in protein levels were measured by normalizing to actin and to total Jnk and dividing the normalized protein level by the mean normalized level in wild-type cells; values are expressed as means (±SD). An asterisk indicates P<0.05 for the comparison with wild type (three to five independent experiments were performed). Panel E shows the analysis of *Sost* mRNA expression in wild-type and *Sfrp4*-null calvarial osteoblasts and bone marrow–derived osteoblasts after 0, 14, and 28 days of osteogenic differentiation. *Sfrp4* deletion affects Sost expression only in calvarial osteoblasts. The bars show mean values; T bars indicate standard deviations. An asterisk indicates P<0.05, and a double asterisk P<0.01 for the comparison with wild type at each time point (three independent

experiments were performed). Panel F shows the regulation of bone morphogenetic protein (BMP) signaling by sFrp4. Wnt5a stimulates *Bmp2* mRNA expression, which was blunted by sFrp4 in MC3T3-E1 cells. The bars show mean values; T bars indicate standard deviations. An asterisk indicates $P<0.05$ for the comparison with control, and a dagger $P<0.05$ for the comparison with Wnt5a-treated cells (three independent experiments were performed). Panel G shows the quantification of *Bmp2* mRNA expression in wild-type and *Sfrp4*-null calvarial osteoblasts and bone marrow–derived osteoblasts. *Sfrp4* deletion affects BMP signaling only in calvarial osteoblasts. The bars show mean values; T bars indicate standard deviations. An asterisk indicates $P<0.05$ for the comparison with wild-type calvarial osteoblasts (three independent experiments were performed). In Panels E, F, and G, fold differences in mRNA expression relative to that in wild-type cells were calculated as described by Livak and Schmittgen.[18] Panel H shows the effects of *Sfrp4* deletion on Smad1, Smad5, and Smad8 phosphorylation, which occurs only in calvarial osteoblasts. We measured fold differences in protein levels by normalizing to Smad1 and dividing the normalized protein level by the mean normalized level in wild-type cells; values are expressed as means (±SD). An asterisk indicates $P<0.05$ for the comparison with wild type (three to five independent experiments were performed). Actin was used as a loading control. Panel I shows representative histologic features of von Kossa–stained tibiae of 3-week-old wild-type and heterozygous mice after vehicle (phosphate-buffered saline) or RAP-661 treatment. Blocking BMP signaling through RAP-661 treatment increases cortical thickness in heterozygous mice (five mice were analyzed in each group). Panel J shows representative images of von Kossa–stained tibiae of wild-type and *Sfrp4*-null male mice treated with a sclerostin-neutralizing antibody (25 mg per kilogram) or vehicle (phosphate-buffered saline) (three to five mice were analyzed in each group). Blocking sclerostin increases cortical thickness in sFrp4-null mice.